Journal of Hazardous Materials 179 (2010) 28–34

Contents lists available at ScienceDirect

Journal of Hazardous Materials

journal homepage: www.elsevier.com/locate/jhazmat

Neutralization of red mud using CO_2 sequestration cycle

Ramesh Chandra Sahu [a], Raj Kishore Patel [a,*], Bankim Chandra Ray [b]

[a] Department of Chemistry, National Institute of Technology, Rourkela 769008, Orissa, India
[b] Department of Metallurgical and Materials Engineering, National Institute of Technology, Rourkela 769008, Orissa, India

ARTICLE INFO

Article history:
Received 11 August 2009
Received in revised form 29 January 2010
Accepted 16 February 2010
Available online 24 February 2010

Keywords:
Red mud
CO_2
Carbonation
Neutralization
FT-IR

ABSTRACT

A laboratory study was conducted to investigate the ability of neutralization of red mud (RM) using carbon dioxide gas sequestration cycle at ambient conditions. The neutralized red mud (NRM) was characterized by XRD, SEM, EDX, FT-IR and auto titration method. X-ray diffraction pattern of NRM was revealed that the intensity of gibbsite was increased prominently and formed ilmenite due to dissolution of minerals. EDX analysis was showed that the %(w/w) of Na, C, O, Si were higher in the carbonated filtrate as compared to the RM and NRM. The permanently sequestered CO_2%(w/w) per 10 g of red mud were ~26.33, ~58.01, ~55.37, and ~54.42 in NRM and first, second, third cycles of carbonated filtrate, respectively. The pH of red mud was decreased from ~11.8 to ~8.45 and alkalinity was decreased from ~10,789 to ~178 mg/L. The acid neutralizing capacity of NRM was ~0.23 mol H^+/kg of red mud. The specific advantages of these cyclic processes are that, large amount of CO_2 can be captured as compared to single step.

1. Introduction

The increase of anthropogenic CO_2 concentration in the atmosphere is creating global challenging problem for future generation. The climate change and global warming can be reduced through utilization of greenhouse gases [1]. CO_2 is a greenhouse gas that makes the largest contribution from human activities. It is released into the atmosphere by the combustion of fossil fuels such as coal, oil or natural gas, and renewable fuels like biomass. CO_2 is an abundant, inexpensive and nontoxic biorenewable resource. It is an attractive raw material for incorporation into important industrial processes [2]. Presently used materials for CO_2 sequestrations are soil [3], steel slags [4], fly ash [5], amine solutions, zeolites, porous membranes, metal-organic frameworks (MOFs) [6], deep geological strata [7].

Red mud (RM) is the caustic waste material of bauxite ore processing for alumina extraction. The Bayer process is commonly used for digestion of bauxite ore in a solution of conc. NaOH at temperatures between 150 and 230 °C under pressure. During the digestion process, aluminum reacts with NaOH to form soluble sodium aluminate leaving red mud slurry [8]. Red mud slurry is highly alkaline having pH > 13, due to presence of NaOH and Na_2CO_3 (1–6%, w/w), these are expressed in terms of Na_2O [9,10]. The main constituents of red mud (% w/w) are: Fe_2O_3 (30–60%), Al_2O_3 (10–20%), SiO_2 (3–50%), Na_2O (2–10%), CaO (2–8%), and TiO_2 (trace–10%) [11].

The main problems of storing red mud slurry are as follows: costly maintenance of large red mud pond areas, risk of caustic for all living organisms, leakage of alkaline compounds into the ground water, overflow of materials and dusting of dry surfaces interfere with nearby rehabilitation on plant life [12,13]. Various methods have been used for neutralization of red mud by adding liquid carbon dioxide [12,14], saline brines or seawater [15], Ca and Mg-rich brines, soluble Ca and Mg salts, acidic water from mine tailing, fly ash, carbon dioxide gas [16,17]. The NRM is utilized for environmental benefits. These processes are costly, so, hardly any industry takes the major to neutralize the red mud. From literature it was cleared that neutralization by using CO_2 showed pH reversion to unaccepted environmental levels as additional alkaline material leaches from the mud.

Utilization of industrial wastes as a resource to solve the problem of another wastes provide economic benefit. The use of CO_2 from the atmosphere or from industrial emissions is another potentially significant source of acid for neutralization of red mud. Since each 500 MW coal power plant emits about 3 million tons of CO_2 per year which may cause serious disruption to the global climate [5]. Red mud is an alkaline waste of alumina industry which can be used as a resource to capture and storage of anthropogenic CO_2, mainly from near source fossil fuel power plants [18]. Neutralization of aqueous caustic red mud solution takes place by the following carbonation reactions of CO_2:

$$CO_2(aq) + OH^-(aq) \leftrightarrow HCO_3^-(aq) \quad (1)$$

$$HCO_3^-(aq) \leftrightarrow H^+(aq) + CO_3^{2-}(aq) \quad (2)$$

$$NaAl(OH)_4(aq) + CO_2(aq) \leftrightarrow NaAl(OH)_2CO_3(s) + H_2O \quad (3)$$

* Corresponding author. Tel.: +91 9437245438; fax: +91 661 2462651.
E-mail addresses: rcsahu.chem@gmail.com (R.C. Sahu), rkpatel@nitrkl.ac.in (R.K. Patel).

0304-3894/$ – see front matter © 2010 Elsevier B.V. All rights reserved.
doi:10.1016/j.jhazmat.2010.02.052

$$3Ca(OH)_2{\bullet}2Al(OH)_3(s) + 3CO_2(aq) \leftrightarrow 3CaCO_3(s) + 2Al(OH)_3(s) + 3H_2O \quad (4)$$

$$Na_6[AlSiO_4]_6{\bullet}2NaOH + 2CO_2(aq) \leftrightarrow Na_6[AlSiO_4]_6 + 2NaHCO_3 \quad (5)$$

With our knowledge from the literature survey, the amount of permanent capture of CO_2 and neutralization of red mud using CO_2 gas up to environmental accepted level has not been reported due to rebound pH. Therefore, the main objective of this study is to investigate the ability of neutralization of caustic red mud using CO_2 sequestration cycle at ambient temperature (24–27 °C) and pressure (1 atm) by simple absorption method. The ultimate aim will also try to find out the permanent capture of CO_2 by reuse of caustic red mud as a low cost absorbent.

2. Materials and methods

2.1. Materials

Fresh red mud used in this study was obtained from R&D Laboratory of NALCO, Damanjodi, Orissa, India, in the form of dried-clay. Hydrochloric acid (HCl) used in this study was of analytical grade and was purchased from Merck. Nitric acid (HNO_3) was purchased from Rankem. Research grade CO_2 (concentration of >99.998% was used without further purification) gas cylinder was purchased from SKP Corporative Service Rourkela. Rotameter was purchased from Bombay Instrument Co.

2.2. Materials preparation

The red mud samples were air-dried and grounded in a mortar and pestle. Subsequently, sieved to pass through a 1 mm sieve, prior to analysis, and stored in vacuum desiccators until used. Particle size of the red mud was in the range of 0.1–160 μm. The red mud suspension was prepared by mixing 10 g of fresh red mud with 100 mL of distilled water in 150 mL plastic bottle to obtain a sufficient volume of slurry for carbonation reaction. The red mud suspensions were kept 24 h with constant magnetic stirring at 180 rpm for standard solid–liquid contact. All these suspensions were prepared in triplicate to get average value.

All the carbonation experiments and measurements were carried out at ambient conditions. All solutions were prepared with distilled water. All plastic sample bottles and glassware were cleaned in 1N HNO_3 acid baths then rinsed with distilled water and dried at 60 °C in a temperature controlled oven.

2.3. Materials characterization

The samples were oven-dried at a temperature of 110 °C for 2 h before their analyses. The XRD pattern of the material and mineral composition were determined by using PHILIPS PANanalytical X'Pert X-ray diffractometer with a Cu Kα radiation source in a 2θ range of 10–90° at a scanning rate of 2° min^{-1}. The surface micro-morphology of materials was investigated using a Scanning Electron Microscope (SEM) and element composition was analyzed using Energy Dispersive X-ray (EDX) by JOEL model JSM-6480LV (Japan). The chemical compositions of major oxides were measured by EDX. These measurements were done in triplicate. FT-IR spectra of the samples were obtained by using PerkinElmer FT-IR Spectrometer Spectrum RX-I. The ratio of sample to KBr was 1:50 and the pallet was prepared at a pressure of 5 tons.

The pH measurements were made using a calibrated Orion 2 Star Bench top pH meter. The electrical conductivities were measured using CM 138, EC-TDS analyzer. The pH and electrical conductivity were measured after centrifugation of suspensions (prepared as indicated in Section 2.2) for 20 min at 3000 rpm and filtration were done using Whatman 40 filter paper. The parameters were measured by adding distilled water to the fresh red mud at a solid to liquid ratio of 1:2.5 standard methods [19]. All these suspensions were prepared in triplicate, and the pH was found ~11.8.

The titrations were done using an Auto Titrator SCHOTT Instrument TitroLine easy (Germany). The acid neutralizing capacities (ANC) of RM and NRM were measured by automatic titration of suspension (mixture of 20.0 g red mud with 50 mL distilled water) with 0.1 M HCl solutions to end point pH 5.5. The titration was repeated after each 24 h until pH becomes stable at 5.5.

The BET surface areas of the samples were measured at liquid nitrogen temperature using BET surface area analyzer (Quantachrome AUTOSORB–1, USA). The BET-N_2 surface area of RM and NRM are 31.7 and 28.55 $m^2\ g^{-1}$ respectively. Particle size of the red mud was measured using Master Sizer 33370-45 (Malverns, UK). Carbon content was determined by using varioELcube CHNS Elemental Analyzer, Germany. The O_2 gas was used as fuel, He gas was used as carrier gas and to provide inert atmosphere. The operating temperature of combustion tube and reduction tube were 1150 and 850 °C, respectively.

2.4. CO_2 sequestration

The CO_2 sequestration reactions were performed at ambient condition at a gas flow rate of 5 mL/min. The reactions were performed in gas tight plastic bottles with an inlet for CO_2 gas and an outlet to vent the pressure. The gas was passed through a rotameter and subsequently passed into the red mud solution through a micro bubbles stone for 5, 10, 20, 24, 48, 72 h. The solution was stirred through a magnetic stirrer at constant speed 180 rpm to increase their solubility for all the experimental tests reported here. The neutralized red mud was collected after a centrifugation for 20 min at 3000 rpm. It was treated as cycle 1 for each carbonation period. The initial and final pH and electrical conductivity were measured according to the technique described in Section 2.3. The alkalinity was measured by using mass balance method [18]. Only 5 h carbonation processes were repeated for cycles 2 and 3.

2.5. Cost estimation

A rough cost is calculated in the SI per ton of CO_2 sequestered in our basic method. Two main components are considered for the cost calculation: electricity for operating magnetic stirrer and centrifuge machine by excluding the cost of machine, plastic bottles, pipes, micro-bobble stone, distilled water, CO_2 used, capital cost, etc. For magnetic stirrer and centrifuge machine energy, it is more convenient to use energy per total mass of CO_2 sequestered, E/M, and then absolute energy [30]:

$$\frac{E}{M} = Pt_s + Pt_c \quad (6)$$

where P is the power, t is the total time of stirring (s) and centrifuge (c). To estimate the CO_2 sequestration cost, T_c, we assume that electricity is purchased at a price, P_{elec}, of $0.07/kW-h according to the year 2008. Applying Eq. (6), we express the sequestration cost by

$$T_c = \frac{P_{elec}E}{M} \quad (7)$$

3. Results and discussion

3.1. Mineralogical characterization by X-ray diffraction

Fig. 1a and b shows the X-ray diffraction patterns of RM and NRM. From the XRD peaks of RM the following mineral phases were

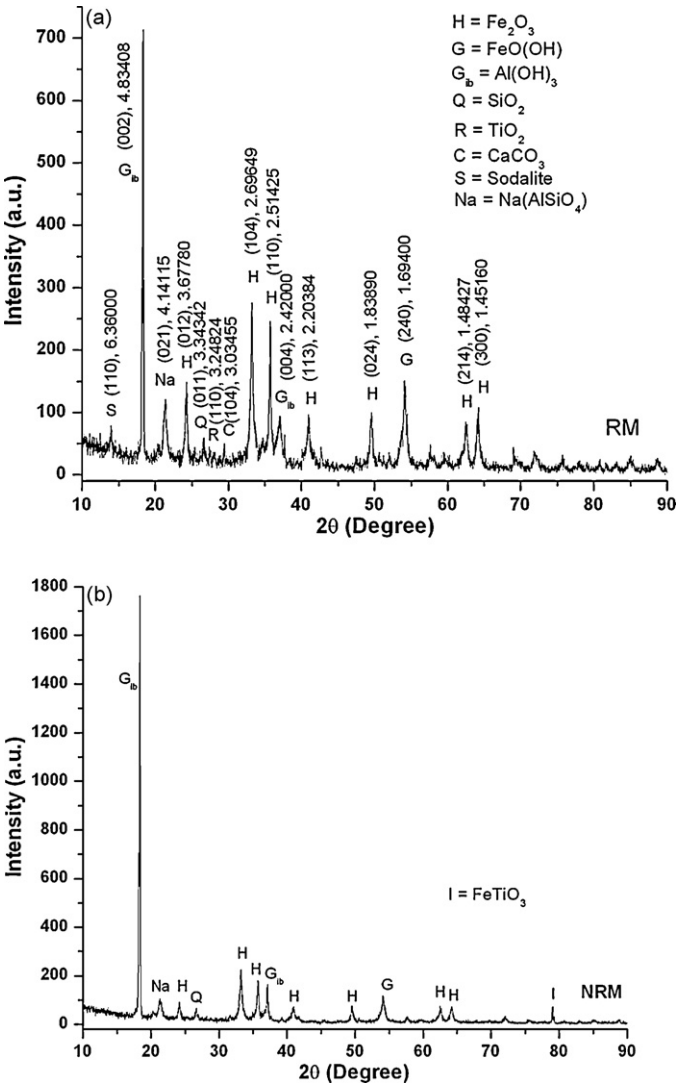

Fig. 1. Variation of powder XRD patterns of (a) RM and (b) NRM.

identified: hematite (α-Fe_2O_3), goethite (α-FeO(OH)), gibbsite (γ-$Al(OH)_3$), calcite ($CaCO_3$), rutile/anatase (TiO_2), sodalite:zeolite (I) ($1.08Na_2OAl_2O_31.68SiO_21.8H_2O$), quartz ($SiO_2$), sodium aluminum silicate ($Na(AlSiO_4)$), and magnetite (Fe_3O_4). XRD pattern of NRM was revealed that the intensity of gibbsite was increased prominently whereas other mineral phases were decreased. Also, confirmed the formation of new mineral ilmenite ($FeTiO_3$). This may be due to dissolution of mineral phases during long period of carbonation. The dissolution of $Na(AlSiO_4)$ is also responsible for increase of intensity of the gibbsite in NRM. It is important to observe that the availability of Na_2O (5.79%, w/w) exceeds the SiO_2 total content (8.45%, w/w). Because, it mainly engaged in $Na(AlSiO_4)$ formation, thus revealing the presence of additional sodium oxide species which is not detected by XRD analysis [20].

3.2. Micro-morphological characterization by SEM and change of chemical composition by EDX

Red mud is a mixture of fine and coarse particles. Fig. 2 shows the particle size distribution of red mud and neutralized red mud. The particle size was decreased after the neutralization experiment from 0.1–160 to 0.1–90 μm. Since, CO_2 is a weak acid, and it helps in dissolution of larger particles. However, CO_2 sequestration decreases with respect to decrease of particle size because CO_2

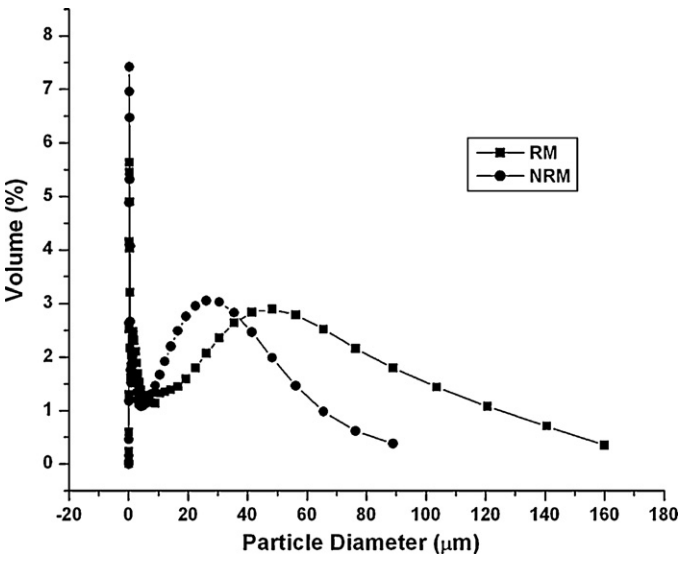

Fig. 2. Particle size distribution of RM and NRM.

Table 1
Major compound composition (%w/w) of RM, NRM and carbonated filtrate of cycles 1, 2, 3 in average as determined by energy dispersive X-ray.

Major oxide	RM	NRM	Carbonated filtrate		
			Cycle 1	Cycle 2	Cycle 3
Fe_2O_3	54.26	47.64	0.00	0.00	0.00
Al_2O_3	12.20	14.37	0.00	0.00	0.00
TiO_2	3.04	3.57	0.00	0.00	0.00
SiO_2	8.45	7.80	1.17	10.11	12.27
Na_2O	5.79	0.29	40.82	34.52	33.31
CaO	0.23	0.00	0.00	0.00	0.00
MgO	0.18	0.00	0.00	0.00	0.00
CO_2	7.23	26.33	58.01	55.37	54.42

sequestration is mainly depends on concentration of NaOH in the red mud. SEM images (Fig. 3a and b) showed that the rounded shape aggregate particles (poorly-crystallized/amorphous forms) present in RM were decreased in the NRM. This indicates that some mineral phases mainly calcite, sodalite contained in the RM are more soluble in acidic environment. However, some silicates often react with sodium aluminate in alkaline solution to form silicate mineral such as hydroxysodalite [8]. SEM images (Fig. 3c–e) revealed the presence of needle morphology in the dried carbonated filtrate this may be due to presence of Na_2CO_3 [21].

The element composition and chemical composition of major oxides were measured by using EDX as in Tables 1 and 2. The samples of carbonated filtrate were dried in water bath at 50 °C to

Table 2
Major element composition (%w/w) of RM, NRM and carbonated filtrate in average as determined by energy dispersive X-ray.

Major element	RM	NRM	Carbonated filtrate		
			Cycle 1	Cycle 2	Cycle 3
C	1.97	7.19	17.93	13.59	11.27
O	31.86	42.40	49.12	53.18	55.08
Na	4.30	0.95	32.75	29.87	26.51
Al	5.86	7.76	0.00	0.00	0.00
Si	3.83	2.18	0.56	3.36	7.14
Ca	0.74	0.00	0.00	0.00	0.00
Ti	1.82	1.60	0.00	0.00	0.00
Fe	47.95	37.92	0.00	0.00	0.00
Zr	1.67	0.00	0.00	0.00	0.00
Total	100.00	100.00	100.00	100.00	100.00

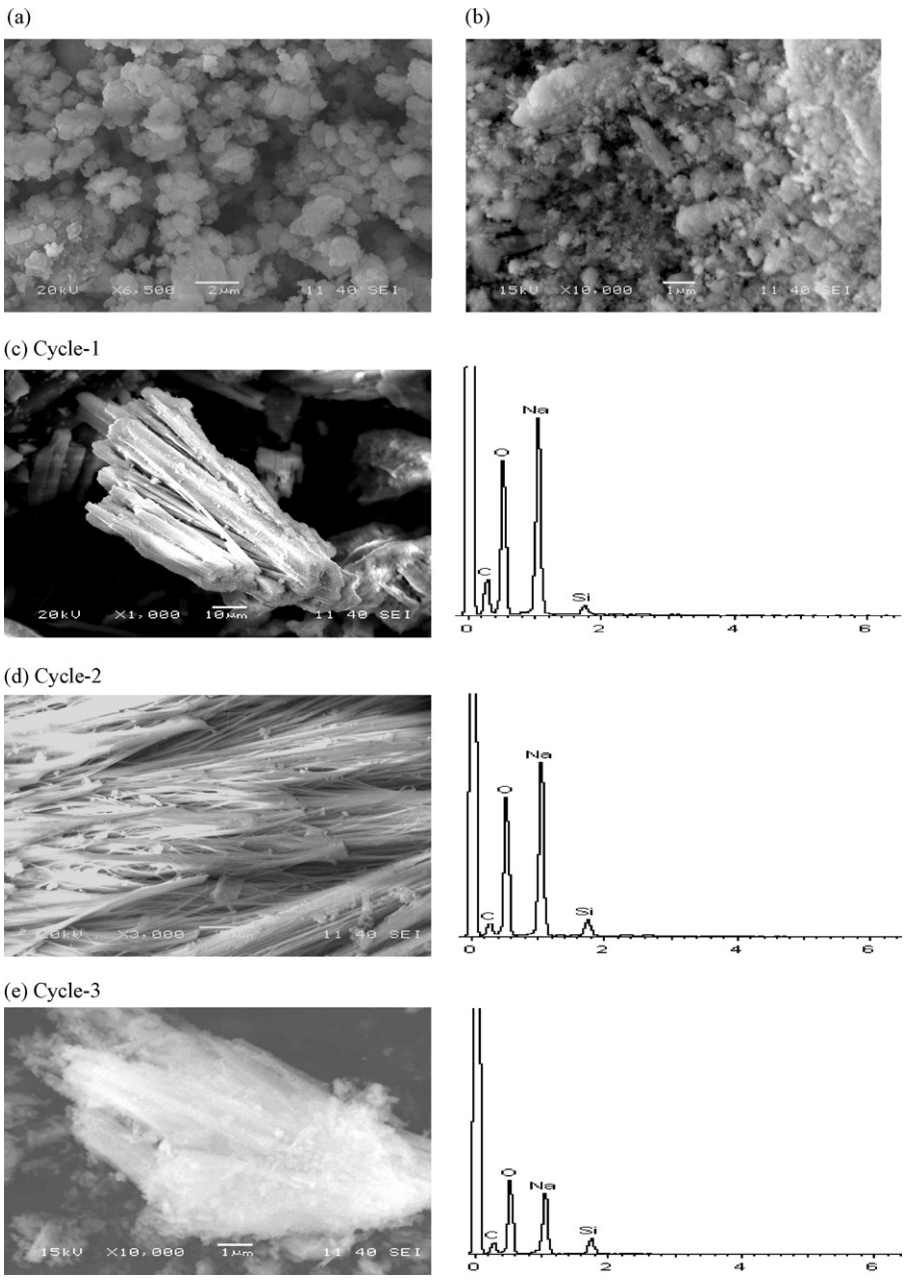

Fig. 3. Variation of SEM micrographs of (a) RM, (b) NRM; and 5 h carbonation filtrate with EDX microanalysis spectrum of (c) cycle 1, (d) cycle 2, and (e) cycle 3.

know the permanent capture of CO_2 and C per 10 g of red mud. The compositions were determined from spot analysis and pallet of the samples. EDX analyses spectra (Fig. 3c–e) revealed that the carbonated filtrate were rich in C (~17.93%), O (~49.12%) and Na (~32.75%) with lower amount of Si (0.56%) in cycle 1. Subsequently, the amount of CO_2 sequestration and leaching of Na^+ ions were decreased, whereas the amount of Si were increased (Tables 1 and 2). Amount of CO_2%(w/w) sequestered permanently in the cycles 1, 2, and 3 were ~58.01, ~55.37, and ~54.42 whereas the amount of C content in each cycle were ~17.93, ~13.59, and ~11.27, respectively. From this it was confirmed that the amount of CO_2 sequestration decreased in each subsequent cycles. The leaching of sodium ions in the cycles 1, 2, and 3 were ~32.75, ~29.87, and ~26.51% (w/w) whereas the compound Na_2O (Na_2CO_3, $NaHCO_3$ and H_2CO_3) was ~40.82, ~43.52, and ~33.31, respectively.

3.3. FT-IR spectroscopy

Fig. 4a shows the FT-IR spectra of RM and NRM. In both the spectra, the positions of the absorption bands are nearly similar. The relative intensities are more intense in the case of RM. The FT-IR absorption by RM was showed a broad band at ~3140 and a weak peak at ~1640 cm^{-1} due to the stretching vibrations of O–H bonds and H–O–H bending vibrations of interlayer adsorbed H_2O molecule, respectively. Water hydroxyl-stretching vibrations are intense in an infrared spectrum, because of large change in dipole moment. The OH-stretching vibrations of carbonated NRM were showed at higher wavenumber at ~3463 cm^{-1}. This shift is associated with the shorter O–H bonds existing in RM than NRM, causing an increase in electrostatic attraction within the RM layer. The absorption bands at ~1476 and ~1489 cm^{-1} are due to stretching vibrations of C═O, confirmed the presence of carbonate groups

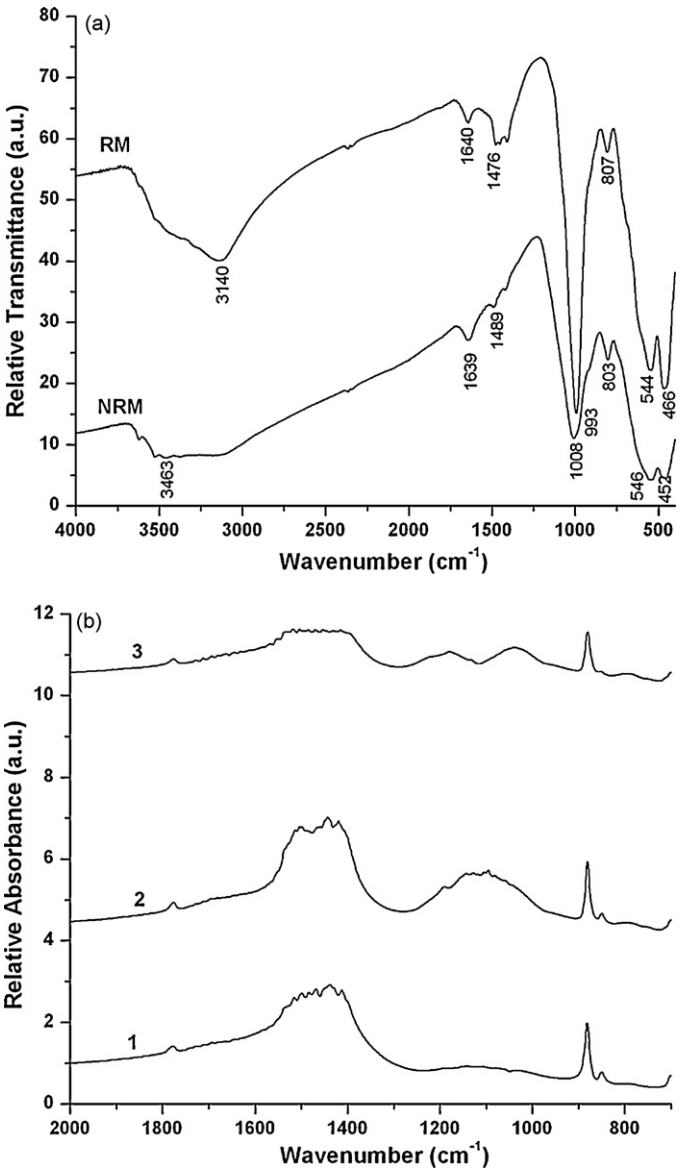

Fig. 4. (a) Variation of FT-IR spectra of RM and NRM. (b) Variation of FT-IR spectra of cycles 1, 2, and 3, each of them treated for 5 h sequestration.

[22]. This may be due to chemisorbed CO_2 in fresh RM and NRM respectively. It confirmed that the fresh red mud was absorbed CO_2 from the atmosphere. Characteristic bands correspond to Si–O vibration were detected at ~993 and ~1008 cm^{-1}, and for O–Si–O at ~803, ~807 cm^{-1} proved the presence of silicate groups. Peaks at ~544 and ~466 cm^{-1} are due to bending vibration of Si–O–Al and stretching vibrations of Fe–O bonds respectively [23,24]. Intensities of these peaks were decreased in NRM which confirmed the dissolution of minerals like silicate, $Na(AlSiO_4)$ during cyclic carbonation.

Fig. 4b shows FT-IR absorption spectrum of carbonated filtrate in the region ~1600–800 cm^{-1}. The vibrational bands at about ~1540, ~1460 and ~875 cm^{-1} are due to CO_3^{2-} [25,26] which confirmed CO_2 sequestration. The broad peaks in between ~1600 and 1200 cm^{-1} are also due to CO_3^{2-} and HCO_3^- [27,28]. Most intense peaks of filtrate at ~1600–1200 and ~875 cm^{-1} indicates sequestration of CO_2 more in filtrate as compared to the suspension. These peaks were more intense in cycles 1 and 2; subsequently decreased in cycle 3, as the amount of CO_2 sequestration decreased. Thus, these ions were formed into stable compounds as Na_2CO_3 and $NaHCO_3$.

3.4. Determination of pH, electrical conductivity and sequestration cycle

The variations of pH, electrical conductivity and alkalinity of RM, carbonated RM are indicated in Fig. 5 and Table 3. The equilibrium pH was achieved in between ~6.8 and ~7.1, mainly due to HCO_3^- ions. Fig. 5a–c shows the rapid decrease of pH, electrical conductivity and alkalinity of RM within 5 h of carbonation, after that rebound slowly. The pH of carbonated slurry rebound again and again, without sequestration cycles. Because, the carbonates were dissolved during equilibrium with the gas phase buffers the water. Also, due to dissolution of alkaline minerals, and as the P_{CO_2} *in situ* is more than atmosphere, so CO_2 moves toward the atmosphere. The pH was decreased from ~11.80 to ~6.81 at the end of cycle 1. The alkalinity was decreased from ~10,789 to ~2583 mg/L. The pH and alkalinity were decreased maximum during 5 h carbonation process. Therefore, neutralization of red mud was done using 5 h carbonation process for subsequent cycles 2 and 3. Ionic solution can sequester CO_2 in a more efficient way. Utilization and sequestration of CO_2 using ionic solution needs less amount of activation energy to form immobilized stable product. Similarly, low viscous solution can dissolve more amounts of alkaline minerals during the long period of carbonation.

The dissociation of Na^+ ions increases the electrical conductivity of the filtrate (Fig. 5b). Complete exchange of Na^+ ions requires longer time of carbonation to reduce the reversible pH. The pH of red mud solution was decreased due to dissolve acidic CO_2, H_2CO_3, CO_3^{2-} and much more in the form of HCO_3^- [29]. The red mud solution rapidly absorbs CO_2 in the form of carbonic acid and neutralizes the excess base in the form of NaOH, Na_2CO_3, $Al(OH)_4^-$. The pH, electrical conductivity and alkalinity of RM after cycle 3 were ~6.33, ~1.41, and ~178 mg/L respectively. Fig. 5d shows that the pH of NRM after cycle 3 was rebound slowly for few days after that it remain constant at 8.45. It is due to presence of some undissolved alkaline minerals. Amount of CO_2 removed for cycles 1, 2, 3 and NRM were 3.54, 2.28, 0.63, 0.57 g CO_2/100 g of red mud, respectively, as determined by CHNS analyzer at 1150 °C. So, total calculated CO_2 removal was 7.02 g/100 g of red mud.

Comparison of CO_2 sequestration capacity of this method with previously used materials by researchers shows the calculated results as: 24.7 g CO_2/100 g of steel slag [4], 2.3 g of CO_2/100 g red mud [12,14], 81 g CO_2/L of MOFs [6], whereas this study shows 7.02 g CO_2/100 g of red mud. The direct comparison among MOFs, steel slag and red mud is difficult because the mechanism of absorption differs completely from adsorption. The sequestration of CO_2 depends on composition of material used. It is expected that CO_2 sequestration using caustic red mud will solve the environmental problem of red mud storage.

3.5. Acid neutralizing capacity (ANC) and cost estimation

Fig. 6 shows that the ANC of RM and NRM were ~1.3 and ~0.23 mol H^+/kg of red mud, respectively. The ANC of NRM was lower due to leaching of strong basic cations Na^+ from carbonated red mud and formation of Na_2CO_3 and $NaHCO_3$.

Cost per unit mass of the CO_2 sequestered (Eq. (7)) highly depend on the amount of electricity. However, the cost of distilled water can be lowered by using normal water. According to the different assumptions about the energy price the cost will varies. Therefore, the roughly calculated cost of CO_2 sequestration is at $147/ton-$CO_2$.

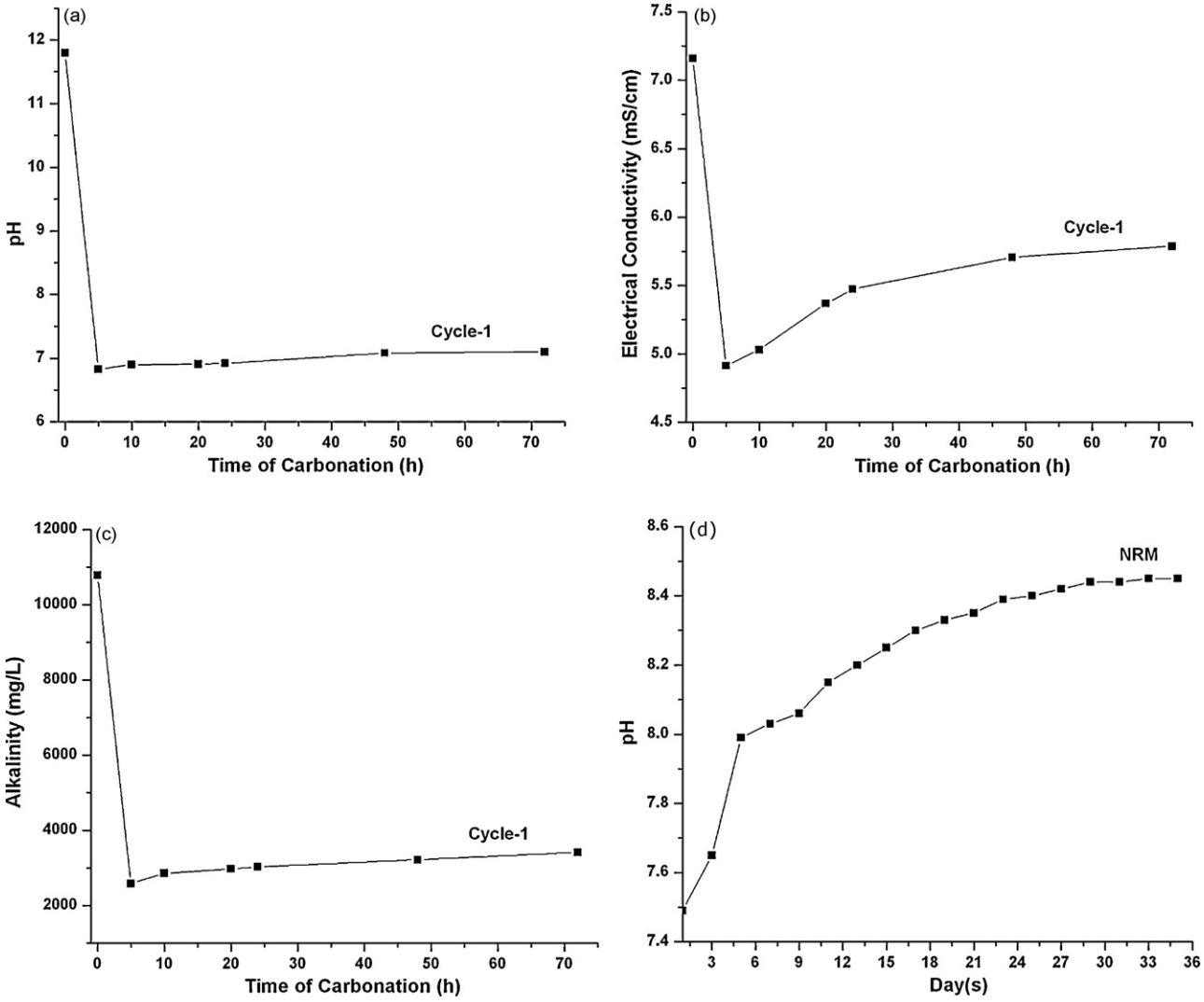

Fig. 5. The average (a) pH, (b) electrical conductivity, (c) alkalinity of carbonated of red mud of cycle 1, and (d) rebound pH of the NRM after cycle 3.

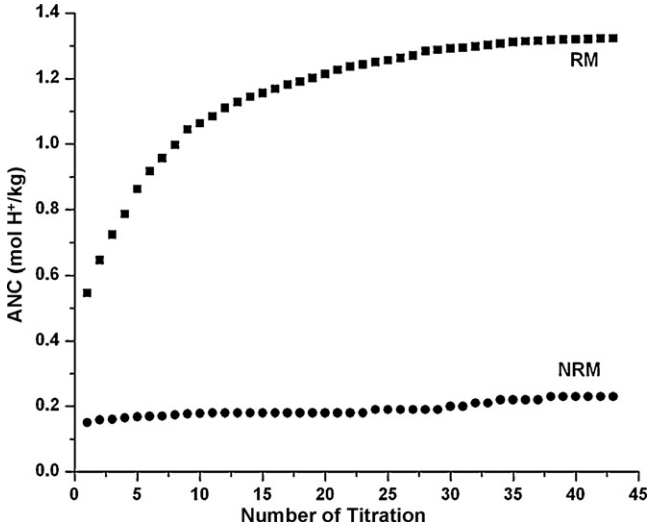

Fig. 6. Variation of acid neutralizing capacity of RM and NRM as obtained by auto titration with 0.1 M HCl solution.

Table 3
The average pH, electrical conductivity, and alkalinity of cycles 1, 2 and 3, each of them treated for 5 h sequestration.

	Cycle 1	Cycle 2	Cycle 3
pH of sequestration	6.81	6.49	6.33
Electrical conductivity (mS/cm)	4.91	2.36	1.41
Alkalinity (mg/L)	2583	834	178

4. Conclusions

In this work caustic red mud was neutralized using CO_2 sequestration cycle. The red mud was treated with CO_2 at 5 mL/min for 5 h in each of the cyclic process. The pH and alkalinity of red mud was decreased from ~11.8 to ~8.45 and ~10,789 to ~178 mg/L at the end of the cycle 3, respectively. The permanently captured CO_2%(w/w) per 10 g of red mud were ~26.33, ~58.01, ~55.37, and ~54.42 in NRM and first, second, third cycles of carbonated filtrate, respectively. The cyclic carbonation was captured more amount of carbon as compared to without cycle. This indicates that caustic filtrate of red mud is more efficient for CO_2 sequestration.

The CO_2 gas was sequestered in the form of Na_2CO_3, $NaHCO_3$, and H_2CO_3 as stable or solid compounds as revealed from FT-IR. The pH rebound of NRM was within the permissible limit of envi-

ronment at the end of the cycles. Hence, utilization of hazardous caustic red mud minerals for sequestration of CO_2 and its neutralization will reduce the environmental problem of red mud storage area. Furthermore, it can solve some problem of global warming.

Acknowledgements

The authors would like to thank "Council of Scientific and Industrial Research" (CSIR, New Delhi, India) for financial support. The authors also thank Prof. S. K. Sarangi, Director, NIT, Rourkela for providing necessary facilities and B. W. Herry (DGM, R&D, NALCO, Damanjodi, India) for providing fresh dried red mud.

References

[1] T.M.L. Wigley, A combined mitigation/geoengineering approach to climate stabilization, Science 314 (2006) 452–454.
[2] D.J. Darensbourg, Making plastic from carbon dioxide: salen metal complexes as catalysts for the production of polycarbonates from epoxides and CO_2, Chem. Rev. 107 (2007) 2388–2410.
[3] R. Lal, Soil carbon sequestration impacts on global climate change and food security, Science 304 (2009) 1623–1627.
[4] D. Bonenfant, L. Kharoune, S. Sauve, R. Hausler, P. Niquette, M. Mimeault, M. Kharoune, CO_2 sequestration potential of steel slags at ambient pressure and temperature, Ind. Eng. Chem. Res. 47 (2008) 7610–7616.
[5] G. Montes-Hernandez, R. Perez-Lopez, F. Renard, J.M. Nieto, L. Charlet, Mineral sequestration of CO_2 by aqueous carbonation of coal combustion fly-ash, J. Hazard. Mater. 161 (2009) 1347–1354.
[6] D. Britt, H. Furukawa, B. Wang, T.G. Glover, O.M. Yaghi, Highly efficient separation of carbon dioxide by a metal-organic framework replete with open metal sites, Proc. Natl. Acad. Sci. U.S.A. 106 (2009) 20637–20640.
[7] S.M.V. Gilfillan, B.S. Lollar, G. Holland, D. Blagburn, S. Stevens, M. Schoell, M. Cassidy, Z. Ding, Z. Zhou, G. Lacrampe-Couloume, C.J. Ballentine, Solubility trapping in formation water as dominant CO_2 sink in natural gas fields, Nature 458 (2009) 614–618.
[8] T. Newson, T. Dyer, C. Adam, S. Sharp, Effect of structure on the geotechnical properties of bauxite residue, J. Geotech. Eng. 132 (2) (2006) 143–151.
[9] H. Genc-Fuhrman, J.C. Tjell, D. McConchie, Increasing the arsenate adsorption capacity of neutralized red mud (bauxsol), J. Colloid Interface Sci. 271 (2004) 313–320.
[10] E. Fois, A. Lallai, G. Mura, Sulfur dioxide absorption in a bubbling reactor with suspensions of Bayer red mud, Ind. Eng. Chem. Res. 46 (2007) 6770–6776.
[11] A. Collazo, M.J. Cristobal, X.R. Novoa, G. Pena, M.C. Perez, Electrochemical impedance spectroscopy as a tool for studying steel corrosion inhibition in simulated concrete environments-red mud used as rebar corrosion, J. ASTM Int. 3 (2) (2006) 1–10.
[12] R.M. Enick, E.J. Beckman, C. Shi, J. Xu, Remediation of metal-bearing aqueous waste streams via direct carbonation, Energy Fuels 15 (2001) 256–262.
[13] C. Brunori, C. Crmisini, P. Massanisso, V. Pinto, L. Torricelli, Reuse of treated red bauxite waste: studies on environmental compatibility, J. Hazard. Mater. B117 (2005) 55–63.
[14] C. Shi, J. Xu, E. Beckman, R. Enick, Carbon dioxide sequestration via pH reduction of red mud using liquid CO_2, ACS Div. Fuel Chem. 45 (4) (2000) 703–705.
[15] C. Hanahan, D. McConchie, P. John, R. Creeiman, M. Clark, C. Stocksiek, Chemistry of sea water neutralization of bauxite refinery residues (red mud), Environ. Eng. Sci. 21 (2004) 125–138.
[16] D. Bonenfant, L. Kharoune, S. Sauve, R. Hausler, P. Niquette, M. Mimeault, M.K. haroune, CO_2 sequestration by aqueous red mud carbonation at ambient pressure and temperature, Ind. Eng. Chem. Res. 47 (2008) 7617–7622.
[17] S. Khaitan, D.A. Dzombak, G.V. Lowry, Mechanisms of neutralization of bauxite residue by carbon dioxide, J. Environ. Eng. 135 (2009) 433–438.
[18] G. Jones, G. Joshi, M. Clark, D. McConichie, Carbon capture and the aluminium industry: preliminary studies, Environ. Chem. 3 (2006) 297–303.
[19] A.F. Bertocchi, M. Ghiani, R. Peretti, A. Zucca, Red mud and fly ash for remediation of mine sites contaminated with As, Cd, Cu, Pb and Zn, J. Hazard. Mater. B 134 (2006) 112–119.
[20] V.M. Sglavo, R.C. ampostrini, S. Maurina, G. Carturan, M. Monagheddu, G. Budroni, G. Cocco, Bauxite red mud in the ceramic industry. Part 1. Thermal behavior, J. Eur. Ceram. Soc. 20 (2000) 235–244.
[21] K.E. Moretto, A process for crystallizing out impurities from Bayer process liquors, European Patent EP0662451 (1999).
[22] C. Cardell, I. Guerra, J. Romero-Pastor, G. Cultrone, A. Rodriguez-Navarro, Innovative analytical methodology combining micro-X-ray diffraction, scanning electron microscopy-based mineral maps, and diffuse reflectance infrared Fourier transform spectroscopy to characterize archeological artifacts, Anal. Chem. 81 (2) (2009) 604–611.
[23] S.J. Palmer, R.L. Frost, T. Nguyen, Hydrotalcites and their role in coordination of anions in Bayer liquors: anion binding in layered double hydroxides, Coord. Chem. Rev. 253 (2009) 250–267.
[24] A. Gok, M. Omastova, J. Prokes, Synthesis and characterization of red mud/polyaniline composites: electrical properties and thermal stability, Eur. Polym. J. 43 (2007) 2471–2480.
[25] P. Regnier, A.C. Lasaga, R.A. Berner, Mechanism of CO_3^{2-} substitution in carbonate-fluorapatite: evidence from FTIR spectroscopy, ^{13}C NMR, and quantum mechanical calculations, Am. Miner. 79 (1994) 809–818.
[26] R.V. Siriwardane, C. Robinson, M. Shen, T. Simonyi, Novel regenerable sodium-based sorbents for CO_2 capture at warm gas temperatures, Energy Fuels 21 (2007) 2088–2097.
[27] L. Meng, S. Burris, H. Bui, W. Pan, Development of an analytical method for distinguishing ammonium bicarbonate from the products of an aqueous ammonia CO_2 scrubber, Anal. Chem. 77 (2005) 5947–5952.
[28] J.A. Tossell, H_2CO_3(s): a new candidate for CO_2 capture and sequestration, Environ. Sci. Technol. 43 (2009) 2575–2580.
[29] G.A. Hill, Measurement of overall volumetric mass transfer coefficients for carbon dioxide in a well-mixed reactor using a pH probe, Ind. Eng. Chem. Res. 45 (2006) 5796–5800.
[30] J.K. Stolaroff, D.W. Keith, G.V. Lowry, Carbon dioxide capture from atmosphere air using sodium hydroxide spray, Environ. Sci. Technol. 42 (2008) 2728–2735.